Table 1 (Continued)

	UPD(14)pat	*Epimutations*	*Microdeletions*				*Total*
			Subtype 1	*Subtype 2*	*Subtype 3*	*Subtotal*	
	Pts 1–23 (n = 23)	*Pts 24–28 (n = 5)*	*Pts 29–31 (n = 3)*	*Pt 32 (n = 1)*	*Pts 33–34 (n = 2)*	*Pts 29–34 (n = 6)*	*Pts 1–34 (n = 34)*
Craniofaciocervical features							
Frontal bossing	17/22	4/5	1/3	1/1	2/2	4/6	25/33
Hairy forehead	18/22	1/5	3/3	1/1	0/2	4/6	23/33
Blepharophimosis	18/22	3/5	2/3	0/1	1/2	3/6	24/33
Small ears	8/21	2/5	1/3	1/1	0/2	2/6	12/32
Depressed nasal bridge	23/23	5/5	3/3	0/1	1/2	4/6	32/34
Anteverted nares	19/22	4/5	3/3	0/1	2/2	5/6	28/33
Full cheek	20/21	4/4	2/2	0/1	1/1	3/4	27/29
Protruding philtrum	23/23	5/5	3/3	0/1	2/2	5/6	33/34
Puckered lips	11/21	3/5	3/3	0/1	0/2	3/6	17/32
Micrognathia	20/21	5/5	3/3	1/1	1/2	5/6	30/32
Short webbed neck	22/22	5/5	3/3	1/1	2/2	6/6	33/33
Thoracic abnormality							
Small bell-shaped thorax in infancy[k]	23/23	5/5	3/3	1/1	2/2	6/6	34/34
Coat-hanger appearance in infancy[l]	23/23	5/5	3/3	1/1	2/2	6/6	34/34
Laryngomalacia	8/20	2/5	2/3	—	0/1	2/4	12/29
Tracheostomy	7/21	1/4	0/2	—	2/2	2/4	10/29
Mechanical ventilation	21/23	5/5	3/3	1/1	2/2	6/6	32/34
Duration of ventilation (m)[m]	1.2 (0.1–17)	0.7 (0.1–0.9)	5 (0.23–10)	—	1.5 (1–2)	2 (0.2–10)	1.0 (0.1–17)
Abdominal wall defects							
Omphalocele	7/23	2/5	1/3	1/1	0/2	2/6	11/34
Diastasis recti	16/23	3/5	2/3	0/1	2/2	4/6	23/34
Developmental delay							
Developmental delay	21/21	5/5	3/3	—	2/2	5/5	31/31
Developmental/intellectual quotient	55 (29–70)	52 (48–56)	Unknown	Unknown	Unknown	—	55 (29–70)
Delayed head control (>4 m)[n]	14/16	4/4	1/1	—	1/1	2/2	20/22
Age at head control (m)[o]	7 (3–36)	7 (6–11)	6	—	6	6 (6)	7 (3–36)
Delayed sitting without support (>7 m)[n]	16/16	4/4	2/2	—	1/1	3/3	23/23
Age at sitting without support (m)[o]	12 (8–25)	11.5 (10–20)	22.5 (18–27)	—	18	18 (18–27)	12 (8–27)
Delayed walking without support (>14 m)[n]	17/17	3/3	2/2	—	2/2	4/4	24/24
Age at walking without support (m)[o]	25.5 (20–49)	25 (22–39)	60 (30–90)	—	24	30 (24–90)	25.5 (20–90)
Other features							
Feeding difficulty	20/21	5/5	3/3	—	2/2	5/5	30/31
Duration of tube feeding (m)[p]	6 (0.1–72)	8.5 (0.5–17)	59.5 (30–89)	—	51	51 (30–89)	7.5 (0.1–89)
Joint contractures	14/22	3/5	3/3	0/1	0/2	3/6	20/33
Constipation	12/20	3/4	1/2	—	0/2	1/4	16/28
Kyphoscoliosis	9/21	3/5	1/2	0/1	0/1	1/4	13/30

Table 1 (Continued)

	UPD(14)pat	*Epimutations*	*Microdeletions*				*Total*
			Subtype 1	*Subtype 2*	*Subtype 3*	*Subtotal*	
	Pts 1–23 (n = 23)	*Pts 24–28 (n = 5)*	*Pts 29–31 (n = 3)*	*Pt 32 (n = 1)*	*Pts 33–34 (n = 2)*	*Pts 29–34 (n = 6)*	*Pts 1–34 (n = 34)*
Coxa valga	6/21	1/5	3/3	0/1	1/2	4/6	11/32
Cardiac disease	5/22	1/5	0/3	1/1	1/2	2/6	8/33
Inguinal hernia	5/22	1/5	2/3	0/1	0/2	2/6	8/33
Seizure	1/21	0/5	0/3	0/1	0/2	0/6	1/32
Hepatoblastoma	3/23	0/5	0/3	0/1	0/2	0/6	3/34
Mortality within the first 5 years							
Alive:deceased	18:5	5:0	2:1	0:1	1:1	3:3	26:8
Parents							
Paternal age at childbirth (y)	35 (24–47)	30 (26–36)	37 (34–39)	25	31.5 (27–36)	35 (25–39)	34 (24–47)
Maternal age at childbirth (y)	31 (25–43)	28 (25–35)	31 (27–36)	25	30.5 (28–33)	29.5 (25–36)	31 (25–43)
Advanced childbearing age (⩾35 y)	8/23	1/5	1/3	0/1	0/2	1/6	8/34

Abbreviations: CHA, coat-hanger angle; Dx, diagnosis; m, month; M/W, mid to widest thorax diameter; UPD(14), uniparental disomy 14; w, week; y, year.
Patient #32 is Irish, and the remaining patients are Japanese; the Irish patient has also been examined by Beygo *et al.*[4]
Age data are expressed by median and range.
The denominators indicate the number of patients examined for the presence or absence of each feature, and the numerators represent the number of patient assessed to be positive for that feature; thus, differences between the denominators and *numeratorsdenote the number of patients evaluated to be negative for the feature.*
[a]For details, see Supplementary Figures S1 and S2.
[b]The *MEG3*-DMR is predicted to be grossly hypomethylated in the placenta.
[c]Expression patterns of the imprinted genes are predicted to be different between the body and the placenta in this patient, while they are predicted to be identical between the body and the placenta in other patients (See Supplementary Figure S1).
[d]Amnioreduction was performed about two times in 23 of the 25 pregnancies.
[e]Placental weight >120% of the gestational age-matched mean placental weight.[34]
[f]The diagnosis of UPD(14)pat has been suspected in two patients (patients #7 and #21).
[g]Birth length and/or birth weight < −2 SD of the gestational age- and sex-matched Japanese reference data (http://jspe.umin.jp/medical/keisan.html).
[h]Birth length and/or birth weight >+2 SD of the gestational age- and sex-matched Japanese reference data (http://jspe.umin.jp/medical/keisan.html).
[i]Present length/height and/or present weight < −2 SD of the age- and sex-matched Japanese reference data (http://jspe.umin.jp/medical/taikaku.html).
[j]Present length/height and/or present weight >+2 SD of the age- and sex-matched Japanese reference data (http://jspe.umin.jp/medical/taikaku.html).
[k]The M/W ratio below nromal range (see Figure 2).
[l]The CHA above the normal range (see Figure 2).
[m]The duration in patients in whom mechanical ventilation could be discontinued.
[n]The age when 90% of infants pass each gross motor developmental milestone (based on Revised Japanese Version of Denver Developmental Screening Test) (http://www.dinf.ne.jp/doc/japanese/prdl/jsrd/norma/n175/img/n175_078i01.gif).
[o]The median (range) of ages in patients who passed each gross motor developmental milestone; patients who have not passed each milestone are not included.
[p]The duration in patients in whom tube feeding could be discontinued.

accompanied by two copies of functional *RTL1* and no functional *RTL1as*.[6] This implies that the *RTL1* expression level is ~2.5 times increased in the absence of functional *RTL1as*-encoded *microRNAs*.

Here, we report comprehensive clinical findings in a series of patients with molecularly confirmed UPD(14)pat and related conditions, and suggest pathognomonic and/or characteristic features and their underlying factors. We also propose the name 'Kagami–Ogata syndrome' for UPD(14)pat and related conditions.

MATERIALS AND METHODS

Ethical approval

This study was approved by the Institute Review Board Committee at the National Center for Child Health and Development, and performed after obtaining written informed consent to publish the clinical and molecular information. We also obtained written informed consent with parental signature to publish facial photographs.

Patients

This study consisted of 33 Japanese patients and one Irish patient (patient #32) with UPD(14)pat and related conditions (13 males and 21 females; 31 patients with normal karyotypes and two patients (#17 and #20) with Robertsonian translocations involving chromosome 14 (karyotyping not performed in patient #1); 30 previously described patients[2,3,7–10] and four new patients) in whom underlying (epi)genetic causes were clarified and detailed clinical findings were obtained (Supplementary Table S2).

The 34 patients were classified into three groups according to the underlying (epi)genetic causes that were determined by methylation analysis for the two DMRs, microsatellite analysis for a total of 24 loci widely dispersed on chromosome 14, fluorescence *in situ* hybridization for the two DMRs, and oligonucleotide array-based comparative genomic hybridization for the 14q32.2 imprinted region, as reported previously:[9] (1) 23 patients with UPD(14)pat (UPD-group); (2) five patients with epimutations (Epi-group); and (3) six patients with microdeletions (Del-group) (Supplementary Figure S2).

Furthermore, the 23 patients of UPD-group were divided into three subtypes in terms of UPD generation mechanisms by microsatellite analysis, as reported previously:[9] (1) 13 patients with monosomy rescue (MR) or postfertilization mitotic error (PE)-mediated UPD(14)pat indicated by full isodisomy (subtype 1) (UPD-S1); (2) a single patient with PE-mediated UPD(14)pat demonstrated by segmental isodisomy (subtype 2) (UPD-S2); and (3) nine patients with trisomy rescue (TR) or gamete complementation (GC)-mediated UPD(14)pat revealed by heterodisomy for at least one locus (subtype 3) (UPD-S3) (Supplementary Figure S2) (it is possible that some patients classified as UPD-S1 may have a cryptic heterodisomic region(s) and actually belong to UPD-S3). Similarly, the six patients of Del-group were divided into three subtypes in terms of the measured/predicted *RTL1* expression level in the body and placenta:[2,3] (1) three patients with ~5 times *RTL1* expression level in both the body and placenta (subtype 1) (Del-S1); (2) a single patient with about five times *RTL1* expression level in the body and normal (1 time) or ~2.5 times *RTL1* expression level in the placenta (subtype 2) (Del-S2); and (3) two patients with ~2.5 times *RTL1* expression level in both the body and placenta (subtype 3) (Del-S3) (Supplementary Figure S2). The measured/predicted expression patterns of the imprinted genes in each group/subtype are illustrated in Supplementary Figure S1.

Clinical studies

We used a comprehensive questionnaire to collect detailed clinical data of all patients from attending physicians. To evaluate chest roentgenographic findings, we obtained the coat-hanger angle (CHA) to the ribs and the ratio of the mid to widest thorax diameter (M/W ratio), as reported previously.[11] We also asked the physicians to report any clinical findings not covered by the questionnaire.

Statistical analysis

Statistical significance of the median among three groups and between two groups/subtypes was examined by the Kruskal–Wallis test and the Mann–Whitney's *U*-test, respectively, and that of the frequency among three groups and between two groups was analyzed by the Fisher's exact probability test, using the R environment (http://cran.r-project.org/bin/windows/base/old/2.15.1/). $P<0.05$ was considered significant. Kaplan–Meier survival curves were constructed using the R environment.

RESULTS

Clinical findings of each group/subtype are summarized in Table 1, and those of each patient are shown in Supplementary Table S2. Phenotypic findings were comparable among UPD-S1, UPD-S2, and UPD-S3, and somewhat different among Del-S1, Del-S2, and Del-S3, as predicted from the expression patterns of the imprinted genes (Supplementary Figure S1). Thus, we showed the data of UPD-group (the sum of UPD-S1, UPD-S2, and UPD-S3) and those of each subtype of Del-group (Del-S1, Del-S2, and Del-S3) in Table 1, and described the data of UPD-S1, UPD-S2, and UPD-S3 in Supplementary Table S3.

We registered the clinical information of each patient in the Leiden Open Variation Database (LOVD) (http://www.lovd.nl/3.0/home; http://databases.lovd.nl/shared/individuals), and the details of each microdeletion in the ClinVar Database (http://www.ncbi.nlm.nih.gov/clinvar/). The LOVD Individual IDs and the ClinVar SCV accession numbers are shown in Supplementary Table S2.

Pregnancy and delivery

Polyhydramnios was observed from ~25 weeks of gestation during the pregnancies of all patients, except for patient #32 of Del-S2 who had deletion of the *MEG3*-DMR and three of the seven *MEG3* exons, and usually required repeated amnioreduction, especially after 30 weeks of gestation. Placentomegaly was usually identified in patients affected with polyhydramnios, but not found in three patients of UPD-group. Thoracic and abdominal abnormalities were found by ultrasound studies in ~40% of patients from ~25 weeks of gestation, and UPD(14)pat was suspected in patients #7 and #21, due to delineation of the bell-shaped thorax with coat-hanger appearance of the ribs. Premature delivery was frequently observed, especially in Del-group. Because of fetal distress and polyhydramnios, ⩾two-thirds of the patients in each group were delivered by Cesarean section. Medically assisted reproduction was reported only in one (patient #8) of 21 patients for whom clinical records on conception were available.

Growth pattern

Prenatal growth was characterized by grossly normal birth length and obviously excessive birth weight. Indeed, birth length ranged from 30.6 to 51.0 cm (−1.7 to +3.0 SD for the gestational age- and sex-matched Japanese reference data) with a median of 44.7 cm (±0 SD), and birth weight ranged from 1.24 to 3.77 kg (+0.1 to +8.8 SD) with a median of 2.79 kg (+2.3 SD). Although birth weight was disproportionately greater than birth length, there was no generalized edema as a possible cause of overweight.

In contrast, postnatal growth was rather compromised, and growth failure (present length/height and/or weight < -2 SD) was observed in about one-third of patients of each group. Postnatal weight was better preserved than postnatal length/height.

Craniofaciocervical features

All patients exhibited strikingly similar craniofaciocervical features (Figure 1). Indeed, >90% of patients had depressed nasal bridge, full cheeks, protruding philtrum, micrognathia, and short webbed neck. In particular, the facial features with full cheeks and protruding philtrum

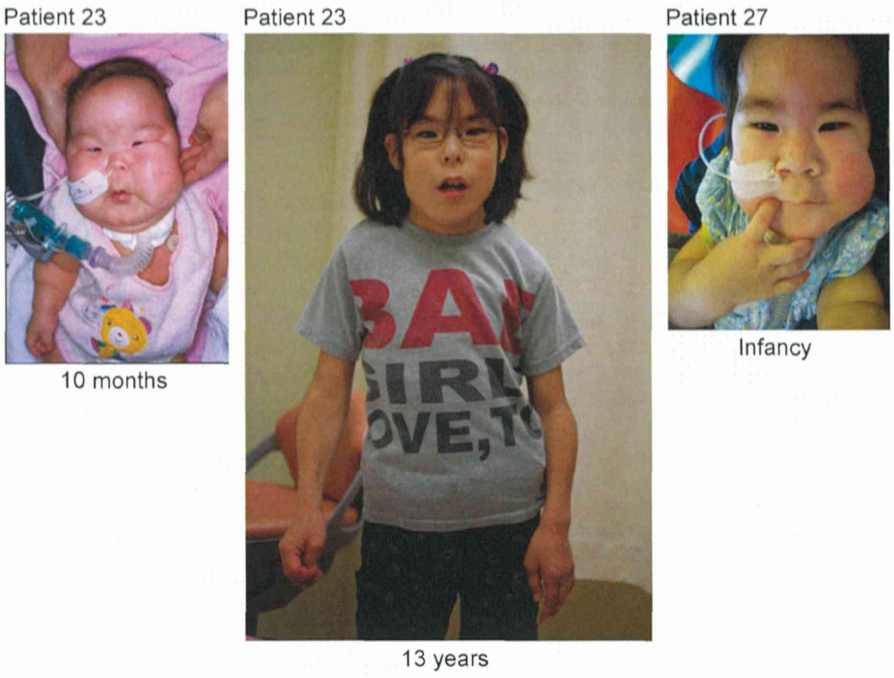

Figure 1 Photographs of patient #23 with UPD(14)pat and patient #27 with epimutation.

appeared to be specific to UPD(14)pat and related conditions, and were recognizable from infancy through childhood.

Thoracic abnormality

The 34 patients invariably showed small bell-shaped small thorax with coat-hanger appearance of the ribs in infancy (Figure 2). Long-term (⩾10 years) follow-up in patient #12 of UPD-group and patient #31 of Del-S1 who had ~5 times of *RTL1* expression, and in patient #34 of Del-S3 who had ~2.5 times of *RTL1* expression, showed that the CHAs remained above the normal range of age-matched control children, while the M/W ratios, though they were below the normal range in infancy, became within the normal range after infancy (Figure 2). Laryngomalacia was also often detected in each group.

Mechanical ventilation was performed in all patients except for patients #14 and #20 of UPD-group, and tracheostomy was also carried out in about one-third of patients. Mechanical ventilation could be discontinued during infancy in 22 patients (Supplementary Figure S3). Ventilation duration was variable with a median period of 1 month among the 22 patients, and was apparently unrelated to the underlying genetic cause or gestational age.

Abdominal wall defects

Omphalocele was identified in about one-third of patients, and diastasis recti was found in the remaining patients.

Developmental status

Developmental delay (DD) and/or intellectual disability (ID) was invariably present in 26 patients examined (age, 10 months to 15 years), with the median developmental/intellectual quotient (DQ/IQ) of 55 (range, 29–70) (Figure 3). Gross motor development was also almost invariably delayed, with grossly similar patterns among different groups. In patients who passed gross motor developmental milestones, head control was achieved at ~7 months, sitting without support at ~12 months, and walking without support at ~2.1 years of age.

Other features

Several prevalent features were also identified. In particular, except for patient #22, feeding difficulty with poor sucking and swallowing was exhibited by all patients who were affected with polyhydramnios, and gastric tube feeding was performed in all patients who survived more than 1 week (Supplementary Figure S4). Tube-feeding duration was variable with a median period of ~7.5 months in 16 patients for whom tube feeding was discontinued, and tended to be longer in Del-group. In addition, there were several features manifested by single patients (Supplementary Table S2).

Notably, hepatoblastoma was identified at 46 days of age in patient #17, at 218 days in patient #18, and at 13 months of age in patient #8 of UPD-group (Figure 4). It was surgically removed in patients #8 and #18, although chemotherapy was not performed because of poor body condition. In patient #17, neither an operation nor chemotherapy could be carried out because of the patient's severely poor body condition. Histological examination of the removed tumors revealed a poorly differentiated embryonal hepatoblastoma with focal macrotrabecular lesions in patient #8 (Figure 4) and a well-differentiated hepatoblastoma in patient #18.[10]

Mortality

Eight patients were deceased before 4 years of age. The survival rate was 78% in UPD-group, 100% in Epi-group, and 50% in Del-group; it was 25% in patients born ⩽29 weeks of gestation, 83% in those born 30–36 weeks of gestation, and 86% in those born ⩾37 weeks of gestation (Figure 5). The cause of death was variable; however, respiratory problems were a major factor, because patient #1 died

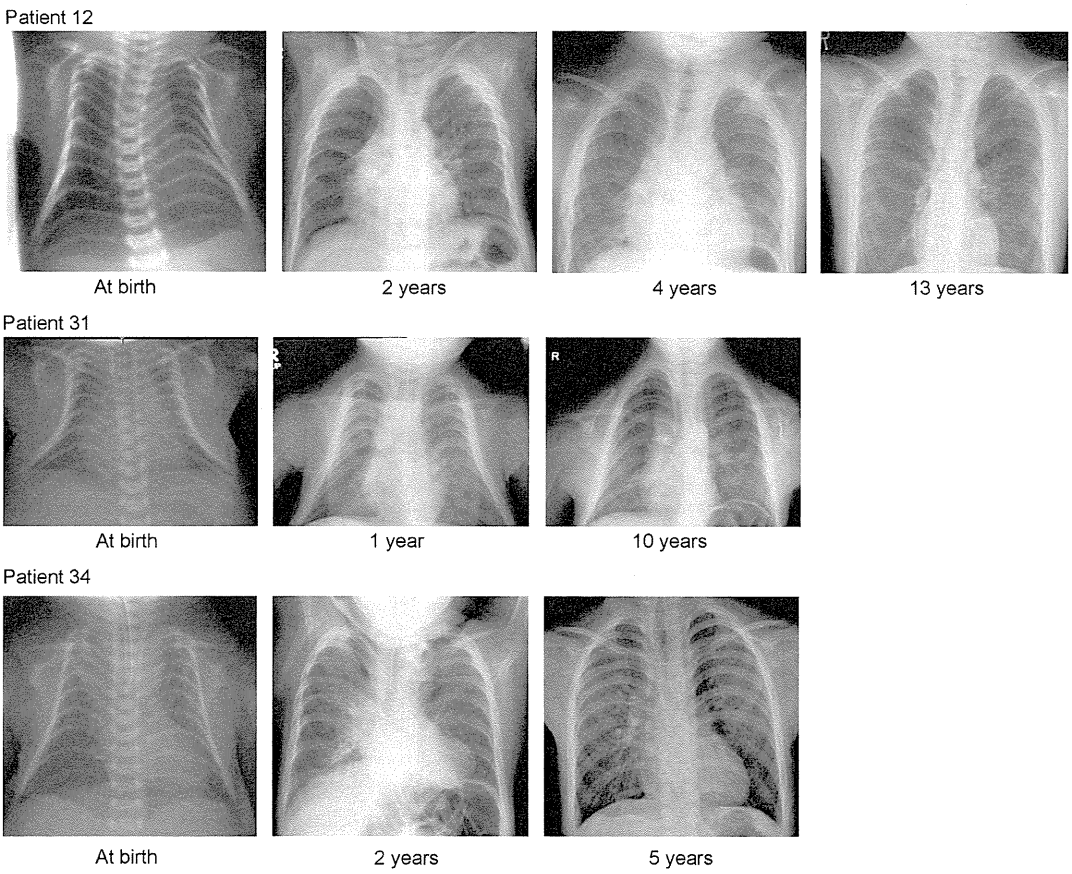

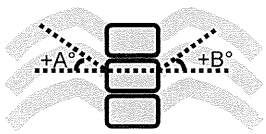

CHA = (A + B) ÷ 2
(6th posterior ribs)

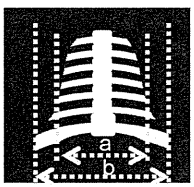

M/W ratio = a / b

		CHA	M/W ratio
Patient 12	At birth	41	70
	2 years	39	88
	4 years	42	94
	13 years	39	92
Patient 31	At birth	35	58
	1 year	28	80
	10 years	29	85
Patient 34	At birth	44	70
	2 year	48	93
	5 years	37	96
UPD(14)pat	At birth	+28 ~ +45	58 ~ 80 (n=8)
	~ 5 years	+25 ~ +45	>78% (n=3)
Controls	At birth	–11 ~ +1.9	82 ~ 89 (n=10)
	~ 5 years	–21 ~ +15	83 ~ 98 (n=10)
	~ 10 years	–9.3 ~ +20	91 ~ 100 (n=10)

Figure 2 Chest roentgenograms of patient #12 of UPD-group, patient #31 of Del-S1, and patient #34 of Del-S3. *RTL1* expression level is predicted to be ~5 times higher in patients #12 and #31, and ~2.5 times higher in patient #34. The CHA to the ribs remains above the normal range throughout the study period, whereas the M/W ratio (the ratio of the mid to widest thorax diameter) normalizes with age.

of neonatal respiratory distress syndrome, and patients #8, #30 and #33 died during a respiratory infection. Of the three patients with hepatoblastoma, patient #17 died of hepatoblastoma, whereas patient #8 died during influenza infection and patient #18 died of hemophagocytic syndrome.

Comparison among/between different groups/subtypes

Clinical findings were grossly similar among/between different groups/subtypes with different expression dosages of *RTL1* and *DLK1*. However, significant differences were found for short gestational age and long duration of tube feeding in Del-group (among three groups

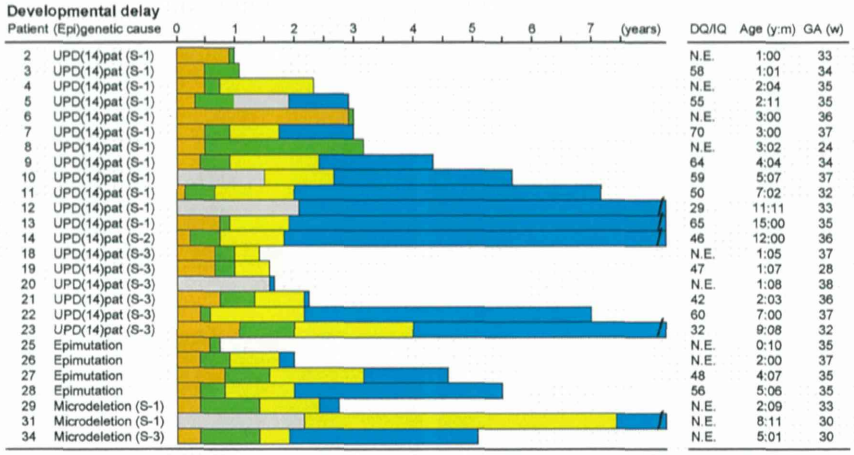

Figure 3 Developmental status. The orange, green, yellow, and blue bars represent the period before head control, the period after head control and before sitting without support, the period after sitting without support and before walking without support, and the period after walking without support, respectively. The gray bars denote the period with no information. DQ, developmental quotient; IQ, intellectual quotient; N.E., not examined; Age, age at the last examination or at death; and GA, gestational age.

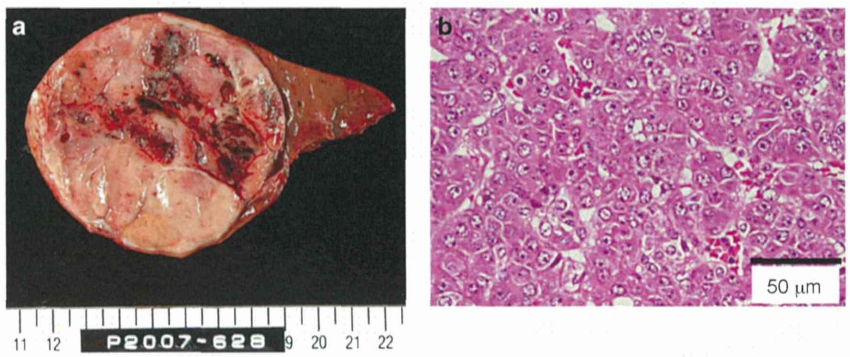

Figure 4 Hepatoblastoma in patient #8 of UPD-group. (**a**) Macroscopic appearance of the hepatoblastoma with a diameter of ~8 cm. (**b**) Microscopic appearance of the hepatoblastoma exhibiting a trabecular pattern. The hepatoblastoma cells are associated with eosinophilic cytoplasm and large nuclei, and resemble fetal hepatocytes.

and against Epi-group and UPD-group) and infrequent hairy forehead in Epi-group (among three groups and against UPD-group) (actual *P*-values are available on request).

DISCUSSION

We examined detailed clinical findings in patients with UPD(14)pat and related conditions. The results indicate that the facial features with full cheeks and protruding philtrum and the thoracic roentgenographic findings with increased CHAs to the ribs represent the pathognomonic features of UPD(14)pat and related conditions from infancy through the childhood. In addition, the decreased M/W ratios also denote the diagnostic hallmark in infancy, but not after infancy. Although other features such as polyhydramnios, placentomegaly, and abdominal wall defects are characteristic of UPD(14)pat and related conditions, they would be regarded as rather nonspecific features that are also observed in other conditions such as Beckwith–Wiedemann syndrome (BWS) (Supplementary Table S4).[12,13]

Such body and placental features were similarly exhibited by patients of each group/subtype, including those of Del-S1, Del-S2, and Del-S3 with different expression dosage of *DLK1* (1× or 2×) and *RTL1* (~2.5× or ~5×), except for patient #32 of Del-S2 who showed typical body features but apparently lacked placental features. Indeed, the difference in the *DLK1* expression dosage had no discernible clinical effects, although mouse *Dlk1* is expressed in several fetal tissues, including the ribs.[14,15] Similarly, in contrast to our previous report which suggested a possible dosage effect of *RTL1* expression level on the phenotypic severity,[2] the difference in the *RTL1* expression dosage turned out to have no recognizable clinical effects after analyzing long-term clinical courses in the affected patients. This suggests that ~2.5×*RTL1* expression is the primary factor for the phenotypic development in the body and placenta. Consistent with the critical role of excessive *RTL1* expression in the phenotypic development, mouse *Rtl1* is clearly expressed in the fetal ribs and skeletal muscles (Supplementary Figure S5) as well as in the placenta,[16,17] and human *RTL1* mRNA and RTL1 protein are strongly expressed in placentas with UPD(14)pat.[6] Thus, lack of placental abnormalities in patient #32 can be explained by assuming a positive *RTL1as* expression and resultant normal (1×) *RTL1* expression in the placenta (Supplementary Figure S1). In addition, since mouse *Gtl2* (*Meg3*) is expressed in multiple fetal tissues including the primordial cartilage,[14] this may argue for the positive role of absent *MEGs* expression in phenotypic development.

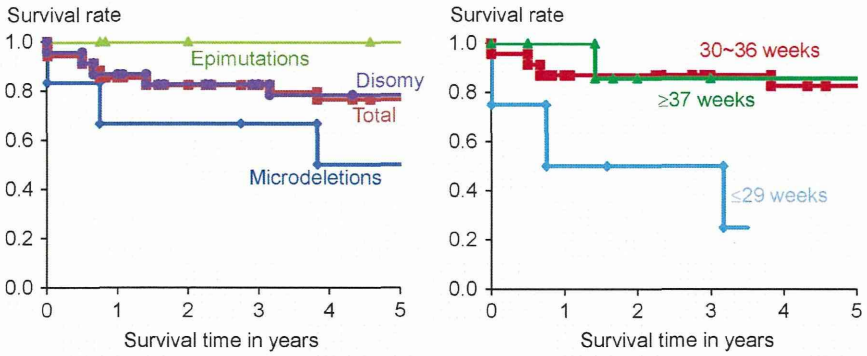

Patient	(Epi)genetic cause	GA	Cause of death	Age of death
1	UPD(14)pat (S-1)	34	Respiratory failure	2 hours
8	UPD(14)pat (S-1)	24	Influenza infection	3 2/12 yrs
15	UPD(14)pat (S-3)	34	Necrotizing enterocolitis	6 mos
17	UPD(14)pat (S-3)	32	Hepatoblastoma	8 mos
18	UPD(14)pat (S-3)	37	Hemophagocytic syndrome	1 5/12 yrs
30	Microdeletion (S-1)	27	Sudden death at URI	9 mos
32	Microdeletion (S-2)	28	Intracranial hemorrhage	4 days
33	Microdeletion (S-3)	35	RS virus infection	3 10/12 yrs

Figure 5 Kaplan–Meier survival curves according to the (epi)genetic cause and the gestational age (week), and summary of the causes of death. GA, gestational age; URI, upper respiratory infection; and RS, respiratory syncytial. Patients #8, #17, and #18 had hepatoblastoma.

The present study revealed several notable findings. First, polyhydramnios was identified during the pregnancies of nearly all patients, except for patient #32 of Del-S2. Amniotic fluid originates primarily from fetal urine and is absorpted primarily by fetal swallowing into the digestive system.[18,19] Since fetal hydration and the resultant urine flow mainly depend on the water flow from maternal circulation across the placenta,[19] placentomegaly would have facilitated the production of amniotic fluid. Furthermore, since feeding difficulty with impaired swallowing was observed in most patients, defective swallowing would have compromised absorption of amniotic fluid. Thus, both body and placental factors are assumed for the development of polyhydramnios. This would explain why polyhydramnios was observed in patients #1, #6, and #8 who were free from placentomegaly, and in patient #22 who showed no feeding difficulty, although the presence of feeding difficulty was unknown for patient #1 as was placentomegaly for patient #22. In addition, since amniotic fluid begins to increase from 8–11 weeks of gestation and reaches its maximum volume around 32 weeks of gestation,[18,19] this would explain why amnioreduction was usually required from 30 weeks of gestation.

Second, birth size was relatively well preserved, whereas postnatal growth was rather compromised. The well preserved prenatal growth in apparently compromised intrauterine environments would be consistent with the conflict theory that overexpression of *PEGs* promotes fetal and placental growth.[20] Notably, birth weight was disproportionately greater than birth length in the apparent absence of generalized edema. In this regard, mouse *Dlk1*, *Rtl1*, and *Gtl2* (*Meg3*) on the distal part of chromosome 12 are expressed in skeletal muscles (Supplementary Figure S5),[14,17] and paternal disomy for chromosome 12 causes muscular hypertrophy.[21] Thus, patients with UPD(14)pat and related conditions may have muscular hypertrophy especially in the fetal life. The compromised postnatal growth would primarily be because of poor nutrition caused by feeding difficulties, whereas relative overweight suggestive of possible muscular hypertrophy remains to be recognized.

Third, DD/ID was invariably present in all 26 patients examined for their developmental/intellectual status, with the median DQ/IQ of 55. In this regard, mouse *Dlk1*, *Rtl1*, and *Gtl2* (*Meg3*) are expressed in the brain during embryogenesis (Supplementary Figure S5),[22] and *Dlk1* is involved in the differentiation of midbrain dopaminergic neurons.[22] Thus, DD/ID would primarily be ascribed to the altered expression dosage of *PEGs/MEGs* in the brain.

Fourth, hepatoblastoma was identified in three patients of UPD-group during infancy. In this context, it has been reported that (1) mouse *Dlk1*, *Rtl1*, and *Meg3* (*Gtl2*) are expressed in the fetal liver, but not in the adult liver; [14,17,23,24] (2) overexpression of *Rtl1* in the adult mouse liver has induced hepatic tumors with high penetrance;[24] (3) *Meg3* functions as a tumor suppressor gene in mice;[25] (4) human *DLK1* is expressed in the hepatocytes of 5–6 weeks old embryos;[26] and (5) human DLK1 protein is upregulated in hepatoblastoma.[27] These findings imply the relevance of excessive *RTL1* expression and loss of *MEG3* expression to the occurrence of hepatoblastoma in UPD(14)pat and related conditions, while it remains to be determined whether the DLK1 upregulation is the cause or the result of hepatoblastoma development. Thus, periodical screening for hepatoblastoma, such as serum α-fetoprotein measurement and abdominal ultrasonography, is recommended. In this context, it remains to be studied whether other embryonal tumors may also be prone to occur in UPD(14)pat and related conditions.

Fifth, mortality was high in Del-group and null in Epi-group. The high mortality in Del-group would primarily be ascribed to the high prevalence of premature delivery, although it is unknown whether the high prevalence of premature delivery is an incidental finding or characteristic of Del-group. The null mortality in Epi-group may be due to possible mosaicism with cells accompanied by a normal expression pattern because of escape from epimutation, as reported previously.[28,29] It is unknown, however, whether possible presence of trisomic cells in TR-mediated UPD(14)pat and that of normal cells in PE-mediated UPD(14) may have exerted clinical effects. Notably, since

death was observed only in patients <4 years of age, the vital prognosis is expected to be good from childhood. In addition, since three patients died during respiratory infections, careful management is recommended during such infections.

Furthermore, the present study also provides several useful clinical implications: (1) two patients had Robertsonian translocations as a risk factor for the development of UPD.[30] Thus, karyotyping is suggested for patients with an UPD(14)pat-like phenotype; (2) prenatal detection of polyhydramnios and thoracic and abdominal features is possible from ~25 weeks of gestation; (3) mechanical ventilation and gastric tube feeding are usually required, with variable durations; (4) there was no patient in UPD-group who exhibited clinical features that are attributable to the unmasking of a recessive mutation(s) of paternal origin; (5) since UPD(14)pat and related conditions share several clinical features including embryonal tumors with BWS (Supplementary Table S4), UPD(14)pat and related conditions may be worth considering in atypical or underlying factor-unknown BWS; and (6) since clinical findings are comparable between patients examined in this study and 17 similarly affected non-Japanese patients (Supplementary Table S5), our data will be applicable to non-Japanese patients as well.

A critical matter for UPD(14)pat and related conditions is the lack of a syndrome name. Although the term 'UPD(14)pat syndrome' has been utilized previously,[4] the term is confusing because 'UPD(14)pat syndrome' can be caused by (epi)genetic mechanisms other than UPD (14)pat. In this regard, the name 'Temple syndrome' has been proposed for UPD(14)mat and related conditions or 'UPD(14)mat syndrome',[31,32] a mirror image of UPD(14)pat and related conditions. On the basis of our previous and present studies that have made a significant contribution to the clarification of underlying (epi)genetic factors and the definition of clinical findings, we would propose the name 'Kagami–Ogata syndrome', or 'Wang–Kagami–Ogata syndrome' with the name of Wang who first described UPD(14)pat,[33] for UPD (14)pat and related conditions.

In summary, although the number of patients still remains small, especially in each subtype of Del-group, the present study reveals pathognomic and characteristic clinical findings in UPD(14)pat and related conditions. Furthermore, this study shows the invariable occurrence of DD/ID and the occasional (8.8%) development of hepatoblastoma, thereby showing the necessity of adequate support for DD/ID and screening of hepatoblastoma in affected patients. Finally, we propose the name 'Kagami–Ogata syndrome' for UPD(14)pat and related conditions.

CONFLICT OF INTEREST

The authors declare no conflict of interest.

ACKNOWLEDGEMENTS

We are grateful to all patients and their parents for their cooperation. We thank Drs Haruhiko Sago, Aiko Sasaki, Jun Shibasaki, Rika Kosaki, Michiko Hayashidani, Toshio Takeuchi, Shinya Tanaka, Mika Noguchi, Goro Sasaki, Kouji Masumoto, Takeshi Utsunomiya, Yumiko Komatsu, Hirofumi Ohashi, Hiroshi Kishimoto, Maureen J O'Sullivan, Andrew J Green, Yoshiyuki Watabe, Tsuyako Iwai, Hitoshi Kawato, Akiko Yamamoto, Nobuhiro Suzumori, Hiroko Ueda, Makoto Kuwajima, Kiyoko Samejima, Hiroshi Yoshihashi, Yoriko Watanabe, Jin Nishimura, Shuku Ishikawa, Michiko Yamanaka, Machiko Nakagawa, Hiroharu Inoue, Takashi Imamura, Keiichi Motoyama and Ryoko Yoshinare for providing us with detailed clinical data and materials for molecular studies, Dr Gen Nishimura for interpretation of roentgengraphic findings, and Drs Tadayuki Ayabe, Keiko Matsubara, Yoichi Sekita and Maki Fukami for their support in molecular analyses. We also thank Ms. Emma Barber for her editorial assistance with the final draft of this paper. This work was supported by Grants-in-Aid for Scientific Research (A) (25253023) and Research (B) (23390083) from the Japan Society for the Promotion of Science (JSPS), and by Grants for Health Research on Children, Youth, and Families (H25-001) and for Research on Intractable Diseases (H22-161) from the Ministry of Health, Labor and Welfare (MHLW), by Grants from the National Center for Child Health and Development (23A-1, 25-10), and by Grant from Takeda Science Foundation.

1 da Rocha ST, Edwards CA, Ito M, Ogata T, Ferguson-Smith AC: Genomic imprinting at the mammalian Dlk1-Dio3 domain. *Trends Genet* 2008; **24**: 306–316.
2 Kagami M, Sekita Y, Nishimura G *et al*: Deletions and epimutations affecting the human 14q32.2 imprinted region in individuals with paternal and maternal upd(14)-like phenotypes. *Nat Genet* 2008; **40**: 237–242.
3 Kagami M, O'Sullivan MJ, Green AJ *et al*: The IG-DMR and the MEG3-DMR at human chromosome 14q32.2: hierarchical interaction and distinct functional properties as imprinting control centers. *PLoS Genet* 2010; **6**: e1000992.
4 Beygo J, Elbracht M, de Groot K *et al*: Novel deletions affecting the MEG3-DMR provide further evidence for a hierarchical regulation of imprinting in 14q32. *Eur J Hum Genet* 2015; **23**: 180–188.
5 Hoffmann K, Heller R: Uniparental disomies 7 and 14. *Best Pract Res Clin Endocrinol Metab* 2011; **25**: 77–100.
6 Kagami M, Matsuoka K, Nagai T *et al*: Paternal uniparental disomy 14 and related disorders: placental gene expression analyses and histological examinations. *Epigenetics* 2012; **7**: 1142–1150.
7 Kurosawa K, Sasaki H, Sato Y *et al*: Paternal UPD14 is responsible for a distinctive malformation complex. *Am J Med Genet* 2002; **110**: 268–272.
8 Kagami M, Nishimura G, Okuyama T *et al*: Segmental and full paternal isodisomy for chromosome 14 in three patients: narrowing the critical region and implication for the clinical features. *Am J Med Genet A* 2005; **138A**: 127–132.
9 Kagami M, Kato F, Matsubara K, Sato T, Nishimura G, Ogata T: Relative frequency of underlying genetic causes for the development of UPD(14)pat-like phenotype. *Eur J Hum Genet* 2012; **20**: 928–932.
10 Horii M, Horiuchi H, Momoeda M, Nakagawa M *et al*: Hepatoblastoma in an infant with paternal uniparental disomy 14. *Congenit Anom (Kyoto)* 2012; **52**: 219–220.
11 Miyazaki O, Nishimura G, Kagami M, Ogata T: Radiological evaluation of dysmorphic thorax of paternal uniparental disomy 14. *Pediatr Radiol* 2011; **41**: 1013–1019.
12 Parveen Z, Tongson-Ignacio JE, Fraser CR, Killeen JL, Thompson KS: Placental mesenchymal dysplasia. *Arch Pathol Lab Med* 2007; **131**: 131–137.
13 Williams DH, Gauthier DW, Maizels M: Prenatal diagnosis of Beckwith–Wiedemann syndrome. *Prenat Diagn* 2005; **25**: 879–884.
14 da Rocha ST, Tevendale M, Knowles E, Takada S, Watkins M, Ferguson-Smith AC: Restricted co-expression of Dlk1 and the reciprocally imprinted non-coding RNA, Gtl2: implications for cis-acting control. *Dev Biol* 2007; **306**: 810–823.
15 da Rocha ST, Charalambous M, Lin SP *et al*: Gene dosage effects of the imprinted delta-like homologue 1 (dlk1/pref1) in development: implications for the evolution of imprinting. *PLoS Genet* 2009; **5**: e1000392.
16 Sekita Y, Wagatsuma H, Nakamura K *et al*: Role of retrotransposon-derived imprinted gene, Rtl1, in the feto-maternal interface of mouse placenta. *Nat Genet* 2008; **40**: 243–248.
17 Brandt J, Schrauth S, Veith AM *et al*: Transposable elements as a source of genetic innovation: expression and evolution of a family of retrotransposon-derived neogenes in mammals. *Gene* 2005; **345**: 101–111.
18 Modena AB, Fieni S: Amniotic fluid dynamics. *Acta Biomed* 2004; **75**: 11–13.
19 Beall MH, van den Wijngaard JP, van Gemert MJ, Ross MG: Amniotic fluid water dynamics. *Placenta* 2007; **28**: 816–823.
20 Hurst LD, McVean GT: Growth effects of uniparental disomies and the conflict theory of genomic imprinting. *Trends Genet* 1997; **13**: 436–443.
21 Georgiades P, Watkins M, Surani MA, Ferguson-Smith AC: Parental origin-specific developmental defects in mice with uniparental disomy for chromosome 12. *Development* 2000; **127**: 4719–4728.
22 Wilkinson LS, Davies W, Isles AR: Genomic imprinting effects on brain development and function. *Nat Rev Neurosci* 2007; **8**: 832–843.
23 Kang ER, Iqbal K, Tran DA *et al*: Effects of endocrine disruptors on imprinted gene expression in the mouse embryo. *Epigenetics* 2011; **6**: 937–950.
24 Riordan JD, Keng VW, Tschida BR *et al*: Identification of rtl1, a retrotransposon-derived imprinted gene, as a novel driver of hepatocarcinogenesis. *PLoS Genet* 2013; **9**: e1003441.
25 Zhou Y, Zhang X, Klibanski A: MEG3 noncoding RNA: a tumor suppressor. *J Mol Endocrinol* 2012; **48**: R45–R53.
26 Floridon C, Jensen CH, Thorsen P *et al*: Does fetal antigen 1 (FA1) identify cells with regenerative, endocrine and neuroendocrine potentials? A study of FA1 in embryonic, fetal, and placental tissue and in maternal circulation. *Differentiation* 2000; **66**: 49–59.
27 Falix FA, Aronson DC, Lamers WH, Hiralall JK, Seppen J: DLK1, a serum marker for hepatoblastoma in young infants. *Pediatr Blood Cancer* 2012; **59**: 743–745.
28 Yamazawa K, Kagami M, Fukami M, Matsubara K, Ogata T: Monozygotic female twins discordant for Silver-Russell syndrome and hypomethylation of the H19-DMR. *J Hum Genet* 2008; **53**: 950–955.

29 Azzi S, Blaise A, Steunou V *et al*: Complex tissue-specific epigenotypes in Russell–Silver Syndrome associated with 11p15 ICR1 hypomethylation. *Hum Mutat* 2014; **35**: 1211–1220.
30 Berend SA, Horwitz J, McCaskill C, Shaffer LG: Identification of uniparental disomy following prenatal detection of Robertsonian translocations and isochromosomes. *Am J Hum Genet* 2000; **66**: 1787–1793.
31 Ioannides Y, Lokulo-Sodipe K, Mackay DJ, Davies JH, Temple IK: Temple syndrome: improving the recognition of an underdiagnosed chromosome 14 imprinting disorder: an analysis of 51 published cases. *J Med Genet* 2014; **51**: 495–501.
32 Hosoki K, Kagami M, Tanaka T *et al*: Maternal uniparental disomy 14 syndrome demonstrates Prader–Willi syndrome-like phenotype. *J Pediatr* 2009; **155**: 900–903.
33 Wang JC, Passage MB, Yen PH, Shapiro LJ, Mohandas TK: Uniparental heterodisomy for chromosome 14 in a phenotypically abnormal familial balanced 13/14 Robertsonian translocation carrier. *Am J Hum Genet* 1991; **48**: 1069–1074.
34 Kagami M, Yamazawa K, Matsubara K *et al*: Placentomegaly in paternal uniparental disomy for human chromosome 14. *Placenta* 2008; **29**: 760–761.

Supplementary Information accompanies this paper on European Journal of Human Genetics website (http://www.nature.com/ejhg)

Endocrine Journal 2014, 61 (9), 849-853

ORIGINAL

Reference standard of penile size and prevalence of buried penis in Japanese newborn male infants

Nobutake Matsuo[1], Tomohiro Ishii[1], John I Takayama[2], Masayuki Miwa[1] and Tomonobu Hasegawa[1]

[1] *Department of Pediatrics, School of Medicine, Keio University, Tokyo, Japan*
[2] *Department of Pediatrics, University of California San Francisco, San Francisco, United States*

Abstract. The present study set forth the reference values for penile size and determined the prevalence of buried penis in Japanese full-term newborns. The stretched penile length was measured and the presence of buried penis was assessed at 1–7 days of age in 547 Japanese full-term newborn infants born between 2008 and 2012 in Tokyo. The stretched penile lengths were compared at 1–12 hours and 1–7 days of age in 63 infants and by two observers in 73 infants to estimate postnatal changes and interobserver variation, respectively. The mean stretched penile length was 3.06 cm (SD, 0.26; 95% confidence interval [CI], 3.04–3.08) and the mean ratio of penile length to body length was 6.24×100^{-1} (SD, 0.55×100^{-1}), both of which were significantly smaller than those in Caucasian newborn infants. Buried penis was identified in 20 of 547 infants (3.7%; 95% CI, 2.1–5.2%). The first measurements of penile length at 1–12 hours were significantly smaller than the next measurements at 1–7 days (95% CI of the difference, 0.22–0.34). The 95% CI for the limits of agreement in the penile lengths measured by the two observers was -0.58 to -0.40 for the lower limit and 0.33 to 0.51 for the upper limit. These findings indicate that the penile length should be assessed after 24 hours of age by the reference standard of the same ethnicity for identifying micropenis and that buried penis is not uncommon in Japanese full-term newborns.

Key words: Stretched penile length, Buried penis, Full-term neonate, Reference value, Ethnicity

PREVIOUS studies indicate that mean penile length is significantly smaller in newborn infants of East Asian origin than in those of Caucasian origin [1-6], although conflicting data have been reported on Singaporean newborn infants [7]. Furthermore, published data on non-Caucasian infants are limited to those assessing Chinese, Saudi Arabian, and East-Indian infants, and relevant data are not available for contemporary Japanese newborn infants. Here, we report the reference standard for penile size to define micropenis in Japanese full-term newborn infants.

Subjects and Methods

A total of 1,210 consecutive full-term newborn infants (610 male and 600 female) were born between January 1, 2008 and December 31, 2012 in a regional hospital in Tokyo. The stretched penile length was measured in 547 of the 610 full-term male newborn infants (Table 1). The inclusion criteria for the study were: (1) 37–42 weeks gestation, (2) 1–7 days of age at measurement, (3) parents of Japanese ethnicity, (4) no cryptorchidism or hypospadias, and (5) no major malformation or chromosomal abnormality. Measurements of stretched penile length were made as a part of the routine physical examination, and the length, weight, head circumference, and placental weight of each infant were measured by the midwives in the nursery. Buried penis was defined as the penis for which the shaft was buried below the surface of the prepubic skin and the stretched length was unmeasurable accurately even with compressing suprapubic fat pad. Baseline demographic data including parity of birth, parental age, parental height and weight, and medical history were also obtained.

Penile length was determined from the pubic ramus to the tip of the glans penis by placing the end of a measuring tape against the pubic ramus and applying traction along the length of the phallus to the point of increased resistance. The stretched penile length

Submitted Feb. 17, 2014; Accepted May 22, 2014 as EJ14-0069
Released online in J-STAGE as advance publication Jun.13, 2014
Correspondence to: Nobutake Matsuo, M.D., Ph.D., Department of Pediatrics, School of Medicine, Keio University, 35 Shinanomachi Shinjuku-ku, Tokyo 160-8582, Japan.
E-mail: nmatsuo@1963.jukuin.keio.ac.jp

Table 1 Stretched penile lengths and demographic characteristics of study subjects (N=547)

	Mean (SD)	Median (SE)	95 % CI
Gestational age (weeks)	39.6 (1.2)	39.7 (0.1)	39.5-39.7
Birth parity	1.6 (0.7)	1 (0.03)	1.5-1.6
Maternal age (years)	31.0 (4.9)	31 (0.2)	30.6-31.4
Paternal age (years)	33.3 (5.7)	33 (0.2)	32.8-33.7
Mid-parental age (years)	32.2 (4.8)	32.3 (0.2)	31.8-32.6
Maternal height (cm)	159.0 (5.4)	159.0 (0.2)	158.6-159.5
Paternal height (cm)	172.3 (5.8)	172.0 (0.2)	171.8-172.7
Mid-parental height (cm)	165.6 (4.1)	165.0 (0.2)	165.3-166.0
Birth weight (g)	3,118 (325)	3,115 (14)	3,091-3,146
Birth length (cm)	49.0 (1.8)	49.0 (0.08)	48.9-49.2
Birth BMI	12.9 (0.9)	13.0 (0.04)	12.9-13.0
Placental weight (g)	582 (103)	570 (4)	574-591
Penile length (cm)	3.06 (0.26)	3.1 (0.01)	3.04-3.08
Standardized penile length (cm/50cm length)	3.12 (0.28)	3.1 (0.01)	3.10-3.14

was measured only for the penis that was fully flaccid. Interobserver agreement was investigated for stretched penile length measurements, using the 95% limits of agreement method by Bland and Altman [8, 9]. Our preliminary study suggested that penile length was shorter if measured soon after birth, since edematous prepubic skin hinders sufficient stretching of the penis. To study the magnitude of the effect of postnatal age of newborn infants on penile size, comparisons were made in 63 infants by using a paired *t*-test for the first measurements obtained within 12 hours of age and the second measurements obtained at 1–7 days of age, each made by the same measurer.

This study was conducted in accordance with the ethical principles set out in the Declaration of Helsinki, and with the ethical guidelines for epidemiological studies issued by the Ministry of Health, Labor and Welfare in Japan.

Results

Mean and SD of penile length

A histogram of penile lengths of Japanese full-term newborn infants is shown in Fig. 1. The mean penile length was 3.06 cm (SD, 0.26 cm), and the 95% confidence interval (CI) was 3.04–3.08 cm. The lower limit of the normal range (-2.5 SD) was 2.40 cm. Thus, micropenis was defined as a penis measuring <2.4 cm in stretched length.

The mean penile length (cm) was divided by the mean body length (cm) at birth to obtain the standardized penile length for full-term newborn infants. The standardized penile length was 6.24×100^{-1} for Japanese infants, whereas it was 6.16×100^{-1} for Canadian Chinese, 6.58×100^{-1} for Canadian Caucasian, 6.74×100^{-1} for Danish and Finnish, and 7.00×100^{-1} for Jewish Israeli infants (unfortunately, body length at birth was not provided for the US Caucasian study).

The coefficient of variation for penile length was 8.5% for Japanese full-term newborn infants, whereas it was 11.4% for Jewish Israeli [5], 11.5% for Danish and Finnish [2], 13.3% for Hong Kong Chinese [6], and 20.0% for American Caucasian [4] full-term newborn infants. This indicates that data on Japanese infants are relatively less spread out as compared to those on infants of other ethnicities.

There was no apparent relationship between gestational age and penile length at 37–42 weeks (Fig. 2), although the correlation coefficient between the weeks of gestation (37–42 weeks) and stretched penile length was 0.12 ($p = 0.004$). We combined the data to derive the reference standard of penile length for Japanese full-term newborn infants.

Interobserver variation

Stretched penile length was measured in 73 infants by two observers to estimate interobserver variation. Differences in the measurements of penile length were plotted against mean penile length by the two observers, with mean difference and 95% limits of agreement indicated (Fig. 3). There was no obvious relationship between the differences and the mean. The differences showed mean and SD values of -0.03 and 0.23, respectively, with the 95% limits of agreement being -0.49

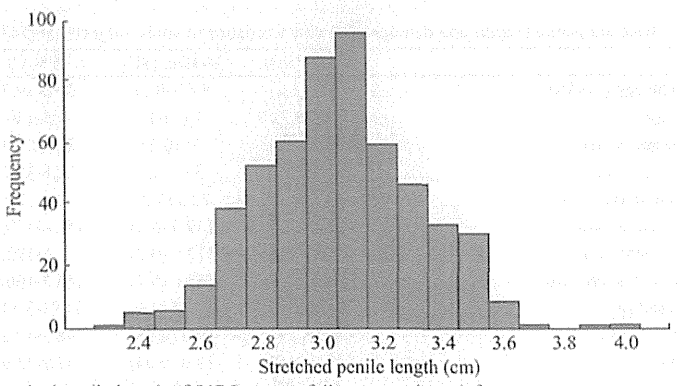

Fig. 1 Histogram of stretched penile length of 547 Japanese full-term newborn infants

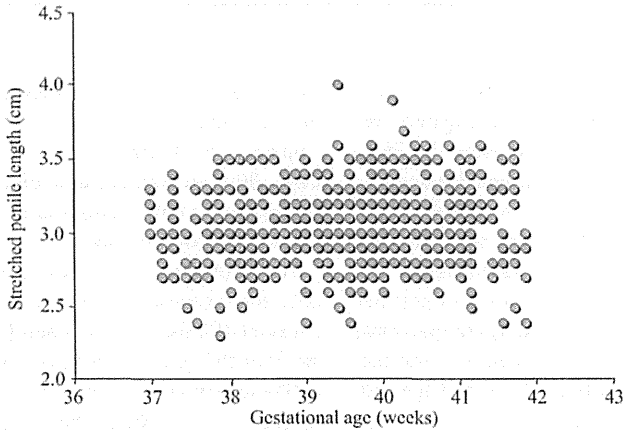

Fig. 2 Stretched penile length according to gestational age. Horizontal axis indicates gestational age in weeks, and vertical axis demonstrates penile length. Dots represent individual measurements

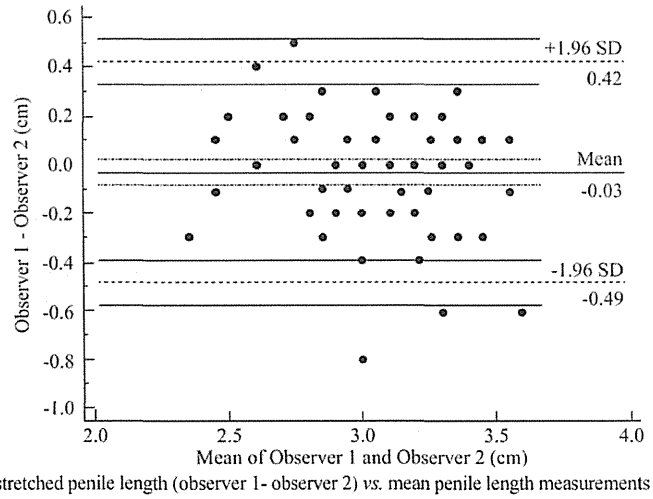

Fig. 3 Differences in stretched penile length (observer 1- observer 2) *vs.* mean penile length measurements made by two different observers

to 0.42. The standard error of the limits was 0.047, as based on the formula $\sqrt{3s^2/n}$, where s is the standard deviation of the differences and n is the sample size. Thus, the 95% CI for the limits of agreement was -0.58 to -0.40 for the lower limit and 0.33 to 0.51 for the upper limit.

Postnatal age at measurement

In 63 full-term newborn infants, penile length was measured first within 12 hours after birth and then at 1–7 days postnatally by the first author. The results are shown in Table 2, which indicate that the first measurements are significantly smaller than the next measurements. Based on these findings, we determined the penile reference standard for full-term newborn infants, as measured at 1–7 days of age.

Buried penis

In buried penis that is obvious at birth, little penile skin is evident and the penile shaft is below the surface of the prepubic skin, which prevents accurate measurement of penile length in infants. Buried penis was diagnosed in 20 of 547 (3.7%) full-term newborn infants, with the 95% CI being 2.1–5.2%. In those 20 infants, the penis was normal in size by palpation, but the stretched penile lengths ranged from 2.3 to 3.1 cm (mean, 2.57). Of the 20 infants diagnosed with buried penis at 1–7 days of age, 12 had buried penis at 1 month, and 8 were lost to follow-up. The 12 infants underwent follow-up for various lengths of time, with 10 having improved or outgrown the condition by 3–4 years of age. The remaining 2 infants continued to have buried penis at 4–5 years of age (0.3%; 95% CI, 0.0–0.9%). We estimate that the prevalence of congenital buried penis in Japanese infants is approximately 2–5% at 1–7 days of age and 0.3% at 4–5 years of age.

Table 2 Stretched penile length measurements in 63 full term newborn infants as determined on two occasions

	1-12 hours of age Mean (SD)	1-7 days of age Mean (SD)	Difference (95%CI)
Penile length	2.75 cm (0.31)	3.03 cm (0.26)	0.30 cm (0.22-0.34)
Age	3.6 hours (3.9)	3.3 days (0.8)	

Discussion

As derived from the present data, the mean stretched penile length for full-term newborn infants was 3.06 cm (SD, 0.26). The lower cutoff limit was calculated to be 2.4 cm (-2.5 SD). These subjects with no sign of disorders of sex development are likely representative of contemporary Japanese newborns, although mild form of androgen insensitivity syndrome [10] or 5α-reductase deficiency [11] cannot be excluded. Thus, micropenis is defined as a penis with a stretched penile length of less than 2.4 cm in contemporary Japanese full-term newborn infants.

The results indicate that the mean penile length is significantly shorter in Japanese newborn infants than in Caucasian newborn infants. The standard reference for penile size has previously been established for American term newborn infants by Feldman and Smith [4], with the mean stretched penile length being 3.5 cm (SD, 0.4). Boas *et al.* [2] also have recently determined new reference ranges for flaccid penile length in Nordic Caucasian newborn infants, with the mean length being 3.49 cm (SD, 0.4). Our finding is in accordance with that of Cheng and Chanoine [3], who documented that the mean penile length is significantly shorter in Canadian newborn infants of Chinese origin than in Canadian newborn infants of Caucasian and East-Indian origins. The mean (SD) was 3.1 (0.3) cm for infants of Chinese ethnicity, 3.4 (0.3) cm for those of Caucasian ethnicity, and 3.6 (0.4) cm for those of East-Indian ethnicity. Fox *et al.* [6] also reported similar data (mean stretched length, 3.0 cm; SD, 0.4 cm) in Hong Kong Chinese full-term newborn infants.

There is no consensus among investigators regarding the standardized method for penile length measurement, i.e., flaccid *vs.* stretched penile length measurements. Schonfeld and Beebe [12] showed that stretched penile length is the most consistent measure of phallic length and that it closely correlates with erect penile length [12]. On the other hand, Boas *et al.* [2] found that flaccid penile length is a reliable measure of phallic length, as an erection is avoided in most cases. Each method obviously has its advantages and disadvantages, as demonstrated by various investigators, but more importantly, Boas *et al.* [2] showed that the standard deviation between the two methods (flaccid *vs.* stretched penile length measurements) was ±0.36 cm, which is comparable to the interobserver variation of ±0.34 cm. This observation indicates that measurements should be repeated in borderline or technically difficult cases, irrespective of whichever method is adopted.

In addition to interobserver variation, we showed that postnatal age at measurement was another source

of measurement variability. The mean penile length measured within 12 hours after birth was 0.31 cm shorter than that re-measured at 1–7 days of age in the 63 infants studied (Table 2). We suspect that smaller penile length readings measured within 12 hours of age reflect edematous prepubic tissue preventing the separation of penopubic tissue from the penis in infants.

To our knowledge, no previous study has addressed the prevalence of buried penis in children or adults. Here, we report that buried penis is not uncommon in Japanese full-term newborn infants, and it occurred in as many as 3–4% of the newborn infants studied. Nevertheless, most newborn infants presented with a mild form of buried penis. They had apparently small penises, but on palpation and by gross estimation, we found that the penises had a normal shaft of normal length. Of the 20 newborn infants with buried penis, only 2 had features of buried penis that lasted till at least 4–5 years of age. Flaccid penile length measurement may be technically problematic in newborn infants with buried penis. Stretched penile length measurement can be performed in such infants, and ultrasound evaluation of penile length may offer a more accurate assessment of functional penile length [13].

We conclude that the micropenis needs to be defined according to ethnicity and a separate penile length be considered as the lowest limit for the definition of micropenis in each population.

Acknowledgments

This work was supported by a Grant-in-Aid for Scientific Research (C) (Grant Number 23591516) from the Japan Society for the Promotion of Science and a Health Science Research Grant for Research on Applying Health Technology (Jitsuyoka (Nanbyo)-Ippan-014) from the Ministry of Health, Labour and Welfare, Japan.

Disclosure

All the authors have no conflict of interest to declare.

References

1. Andersson A-M, Toppari J, Haavisto AM, Petersen JH, Simell T, et al. (1998) Longitudinal reproductive hormone profiles in infants: peak of inhibin B levels in infant boys exceeds levels in adult men. *J Clin Endocrinol Metab* 83: 675-681.
2. Boas M, Boisen K, Virtanen H, Kaleva M, Suomi A, et al. (2006) Postnatal penile length and growth rate correlate to serum testosterone levels: a longitudinal study of 1962 normal boys. *Eur J Endocrinol* 154: 125-129.
3. Cheng PK, Chanoine JP (2001) Should the definition of micropenis vary according to ethnicity? *Horm Res* 55: 278-281.
4. Feldman KW, Smith DW (1975) Fetal phallic growth and penile standards for newborn male infants. *J Pediatr* 86: 395-398.
5. Flatau E, Josefsberg Z, Reisner SH, Bialik O, Iaron Z (1975) Letter: Penile size in the newborn infant. *J Pediatr* 87: 663-664.
6. Fok TF, Hon KL, So HK, Wong E, Ng PC, et al. (2005) Normative data of penile length for term Chinese newborns. *Biol Neonate* 87: 242-245.
7. Lian WB, Lee WR, Ho LY (2000) Penile length of newborns in Singapore. *J Pediatr Endocrinol Metab* 13: 55-62.
8. Bland JM, Altman DG (1986) Statistical methods for assessing agreement between two methods of clinical measurement. *Lancet* 1: 307-310.
9. Bland JM, Altman DG (2003) Applying the right statistics: analyses of measurement studies. *Ultrasound Obstet Gynecol* 22: 85-93.
10. Ishii T, Sato S, Kosaki K, Sasaki G, Muroya K, et al. (2001) Micropenis and the AR gene: mutation and CAG repeat-length analysis. *J Clin Endocrinol Metab* 86: 5372-5378.
11. Sasaki G, Ogata T, Ishii T, Kosaki K, Sato S, et al. (2003) Micropenis and the 5 -reductase-2 (SRD5A2) gene: mutation and V89L polymorphism analysis in 81 Japanese patients. *J Clin Endocrinol Metab* 88: 3431-3436.
12. Schonfeld WA, Beebe GW (1942) Normal growth and variation in the male genitalia from birth to maturity. *J Urol* 48: 759-777.
13. Smith DP, Rickman C, Jerkins GR (1995) Ultrasound evaluation of normal penile (corporeal) length in children. *J Urol* 154: 822-824.

OPEN ACCESS Freely available online

PLOS | ONE

TBX1 Mutation Identified by Exome Sequencing in a Japanese Family with 22q11.2 Deletion Syndrome-Like Craniofacial Features and Hypocalcemia

Tsutomu Ogata[1*☯], Tetsuya Niihori[2☯], Noriko Tanaka[3☯], Masahiko Kawai[4], Takeshi Nagashima[5], Ryo Funayama[5], Keiko Nakayama[5], Shinichi Nakashima[1], Fumiko Kato[1], Maki Fukami[6], Yoko Aoki[2], Yoichi Matsubara[2,6]

1 Department of Pediatrics, Hamamatsu University School of Medicine, Hamamatsu, Japan, **2** Department of Medical Genetics, Tohoku University School of Medicine, Sendai, Japan, **3** Department of Pediatrics, Kurashiki Central Hospital, Kurashiki, Japan, **4** Department of Pediatrics, Kyoto University School of Medicine, Kyoto, Japan, **5** Division of Cell Proliferation, United Centers for Advanced Research and Translational Medicine, Tohoku University Graduate School of Medicine, Sendai, Japan, **6** National Research Institute for Child Health and Development, Tokyo, Japan

Abstract

Background: Although *TBX1* mutations have been identified in patients with 22q11.2 deletion syndrome (22q11.2DS)-like phenotypes including characteristic craniofacial features, cardiovascular anomalies, hypoparathyroidism, and thymic hypoplasia, the frequency of *TBX1* mutations remains rare in deletion-negative patients. Thus, it would be reasonable to perform a comprehensive genetic analysis in deletion-negative patients with 22q11.2DS-like phenotypes.

Methodology/Principal Findings: We studied three subjects with craniofacial features and hypocalcemia (group 1), two subjects with craniofacial features alone (group 2), and three subjects with normal phenotype within a single Japanese family. Fluorescence *in situ* hybridization analysis excluded chromosome 22q11.2 deletion, and genomewide array comparative genomic hybridization analysis revealed no copy number change specific to group 1 or groups 1+2. However, exome sequencing identified a heterozygous *TBX1* frameshift mutation (c.1253delA, p.Y418fsX459) specific to groups 1+2, as well as six missense variants and two in-frame microdeletions specific to groups 1+2 and two missense variants specific to group 1. The *TBX1* mutation resided at exon 9C and was predicted to produce a non-functional truncated protein missing the nuclear localization signal and most of the transactivation domain.

Conclusions/Significance: Clinical features in groups 1+2 are well explained by the *TBX1* mutation, while the clinical effects of the remaining variants are largely unknown. Thus, the results exemplify the usefulness of exome sequencing in the identification of disease-causing mutations in familial disorders. Furthermore, the results, in conjunction with the previous data, imply that *TBX1* isoform C is the biologically essential variant and that *TBX1* mutations are associated with a wide phenotypic spectrum, including most of 22q11.2DS phenotypes.

Citation: Ogata T, Niihori T, Tanaka N, Kawai M, Nagashima T, et al. (2014) *TBX1* Mutation Identified by Exome Sequencing in a Japanese Family with 22q11.2 Deletion Syndrome-Like Craniofacial Features and Hypocalcemia. PLoS ONE 9(3): e91598. doi:10.1371/journal.pone.0091598

Editor: Reiner Albert Veitia, Institut Jacques Monod, France

Received November 12, 2013; **Accepted** February 12, 2014; **Published** March 17, 2014

Funding: This work was supported in part by grants from the Ministry of Health, Labor, and Welfare, from the Ministry of Education, Culture, Sports, Science and Technology, and from the National Center for Child Health and Development. The funders had no role in study design, data collection and analysis, decision to publish, or preparation of the manuscript.

Competing Interests: The authors have declared that no competing interests exist.

* E-mail: tomogata@hama-med.ac.jp

☯ These authors contributed equally to this work.

Introduction

Chromosome 22q11.2 deletion syndrome (22q11.2DS) is a developmental disorder associated with characteristic craniofacial features with velopharyngeal incompetence, cardiovascular anomalies primarily affecting the outflow tracts, hypoparathyroidism and resultant hypocalcemia, and thymic hypoplasia leading to susceptibility to infection [1]. This condition is also frequently accompanied by non-specific clinical features such as developmental retardation [1]. Expressivity and penetrance of these features are highly variable and, consistent with this, chromosome 22q11.2 deletions have been identified in DiGeorge syndrome (DGS) and velocardiofacial syndrome (VCFS) with overlapping but different patterns of clinical features [1].

While multiple genes are involved in chromosome 22q11.2 deletions [2], *TBX1* (T-box 1) has been regarded as the major gene relevant to the development of clinical features in 22q11.2DS [3]. Indeed, heterozygous *TBX1* mutations have been identified in several deletion-negative patients with 22q11.2DS phenotype [2–8], and mouse studies argue for the critical role of *Tbx1* in the development of 22q11.2DS phenotypes [3]. However, the frequency of *TBX1* mutations remains rare in deletion-negative patients: Gong et al. identified only a few probable *TBX1* mutations after studying 40 patients with DGS/VCFS phenotypes

[4], and Zweier et al. found a single *TBX1* mutation after examining 10 patients with 22q11.2DS phenotype [8]. This indicates the presence of genetic heterogeneity in the development of 22q11.2DS phenotype in deletion-negative patients. Consistent with this, another DGS/VCFS locus has been assigned to chromosome 10p13-14 region [9]. Thus, it would be reasonable to perform a comprehensive genetic analysis in deletion-negative patients with 22q11.2DS phenotype.

In this regard, recent advance in molecular technologies has enabled to perform comprehensive genetic analyses, thereby contributing to the identification of underlying factors in genetic disorders. Indeed, genomewide array comparative genomic hybridization (CGH) has identified multiple disease-associated copy-number changes [10], and exome sequencing has discovered multiple disease-causing gene mutations [11]. In particular, these technologies can be powerful methods for familial disorders, because it is predicted that a single copy-number change or mutation is shared in common by affected subjects and is absent from non-affected subjects within a family.

Here, we performed array CGH analysis and exome sequencing in a family with 22q11.2DS-like clinical features. Although this study did not discover a novel disease gene, a *TBX1* mutation was successfully identified.

Materials and Methods

Ethics statement

The Institutional Review Board Committees of Hamamatsu University School of Medicine, Tohoku University School of Medicine, Kurashiki Central Hospital, and National Research Institute for Child Health and Development considered and approved the study, consent/assent procedures, and the publication of images and case details associated with this work. The individuals in this manuscript have given written informed consent (as outlined in PLOS consent form) to publish these case details. Actually, this study was performed after obtaining written informed consent from the parents of the child subjects and from the adult subjects. Furthermore, the mother and the elder brother aged 19 years old have given written informed consent to publication of the facial photographs of the two brothers; in addition, the younger brother aged 10 years has given informed assent.

Clinical Report

The pedigree of this Japanese family is shown in Fig. 1, and clinical findings of the family members are summarized in Table 1. The proband (subject III-5) was found to have hypocalcemia and hyperphosphatemia in a pre-operation laboratory test for repeated otitis media at 8 years of age, and was referred to Department of Pediatrics at Kurashiki Central Hospital. Subsequent examination revealed borderline low serum intact PTH value. Thus, he was diagnosed as having hypoparathyroidism, and received vitamin D therapy. Furthermore, physical examination showed characteristic craniofacial features with velopharyngeal incompetence suggestive of 22q11.2DS.

Similar craniofacial features were also exhibited by subjects II-2, III-1, III-6, and III-7, and hypocalcemia was also identified in subjects II-2 and III-7. Actually, subject II-2 was taking vitamin D, and subject III-7 was noticed to have hypocalcemia at birth because of the history of subject III-5, and was treated with vitamin D. The five subjects with 22q11.2DS-like craniofacial features lacked cardiovascular anomalies; while they also lacked susceptibility to infection, except for repeated otitis media in subject III-5, thymic hypoplasia was not evaluated in four of the five subjects. By contrast, the five subjects exhibited borderline to mild developmental delay. Indeed, adult subjects II-2 and III-1 had some difficulty in verbal communications, although they were able to get on their daily life, and subject II-2 was able to take care of family members. Similarly, child subjects III-5, III-6, and III-7 also showed speech delay, and subjects III-5 and III-7 received speech therapy. Furthermore, subject III-7 was diagnosed as having pervasive developmental disorder, and his verbal, performance, and full scale intelligence quotients were assessed as 63, 64, and 60, respectively, by the WISC-III method at 10 years of age. In addition, subject II-2 had sensorineural deafness, and subject III-5 had Graves' disease.

Molecularly Studied Subjects

Molecular studies were performed for eight subjects in this family, using peripheral blood samples. They were divided into three groups in terms of clinical findings: group 1, subjects II-2, III-5, and III-7 with craniofacial features and hypocalcemia; group 2, subjects III-1 and III-6 with craniofacial features alone; and group 3, subjects II-1, III-3, and IV-1 with apparently normal phenotype (Fig. 1).

FISH and Array CGH Analyses

Fluorescence *in situ* hybridization (FISH) analysis was performed with a probe for *HIRA* on the commonly deleted chromosome 22q11.2 region and that for *ARSA* at chromosome 22q13 utilized as an internal control (Abott). Array CGH was carried out using a genomewide 2x400K Agilent platform catalog array, according to the manufacturer's instructions (Agilent Technologies), and copy number variants/polymorphisms were screened with Agilent Genomic Workbench software using the Database of Genomic Variants (http://dgv.tcag.ca/dgv/app/home).

Exome and Sanger Sequencings

Exon capture was performed with the SureSelect Human All Exon kit v4 (Agilent Technologies). Exon libraries were sequenced with the Illumina Hiseq 2000 platform according to the manufacturer's instructions (Illumina), providing 108–122 average depth for each sample. Paired 101-base pair reads were aligned to the reference human genome (UCSChg19) using the Burrows-Wheeler Alignment tool [12]. Likely PCR duplicates were removed with the Picard program (http://picard.sourceforge.net/). Single-nucleotide variants and indels were identified using the Genome Analysis Tool Kit (GATK) v1.6 software [13]. SNVs and indels were annotated against the RefSeq database, 1000 Genomes Project variant data, and dbSNP135 with the ANNOVAR program [14].

To confirm mutations indicated by exome sequencing, Sanger sequencing was performed for PCR products obtained with primers flanking the detected mutations, using a 3500xL genetic analyzer (Life Technologies). Furthermore, the PCR products were subcloned with TOPO TA Cloning Kit (Life Technologies), and normal and mutant alleles were sequenced separately.

In silico protein functional analysis

Function of proteins with missense variations was assessed by Polymorphism Phenotyping-2 (PolyPhen-2, http://genetics.bwh.harvard.edu/pph2/) and Sorting Intolerant From Tolerant (SIFT, http://sift.jcvi.org/), and that of proteins with in-frame amino acid deletions was evaluated by PROVEAN predictions (http://provean.jcvi.org/index.php).

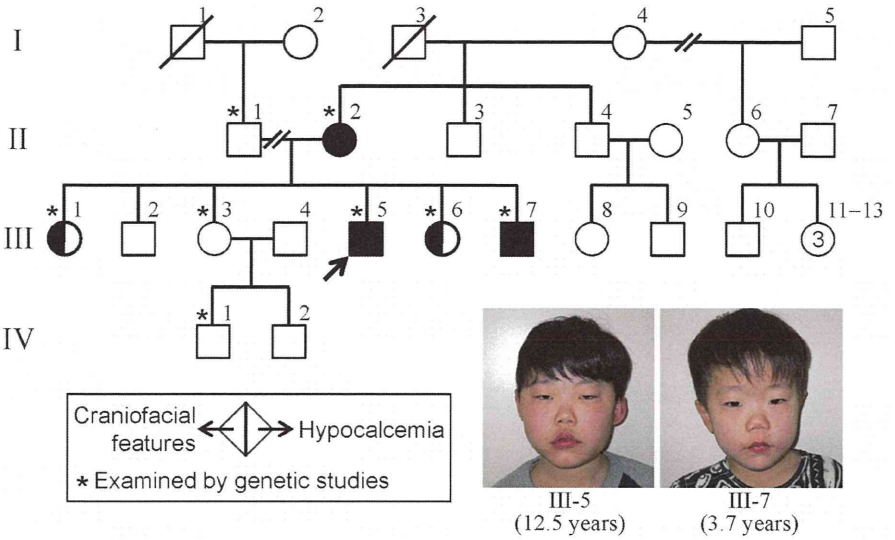

Figure 1. The pedigree of this family. Facial features of subjects III-5 and III-7 are shown.
doi:10.1371/journal.pone.0091598.g001

Results

FISH and Array CGH Analyses

FISH analysis delineated two signals for *HIRA* (Fig. 2A). Array CGH analysis revealed no copy number change specific to group 1 or groups 1+2, in the entire genome including chromosome 10p13-14 and chromosome 22q11.2 regions (Fig. 2B).

Exome and Sanger Sequencings

Exome sequencing identified nine heterozygous non-synonymous variants (six missense variants, two in-frame microdeletions, and one frameshift variant) that were specific to groups 1+2 (namely, they were present in groups 1+2 and absent from group 3 as well as from 1000 Genomes, dbSNP135, and our in-house exome data from 70 individuals) (Table S1). Notably, the frameshift variant (c.1253delA, p.Y418fsX459) was found at exon 9C of *TBX1* for DGS/VCFS (Fig. 3). Of the remaining eight variants, two variants were also detected in disease-related genes: p.G204R in *HDAC4* for brachydactyly-mental retardation syndrome [15], and p.276del in *CCND1* constituting a susceptibility factor for colorectal cancer and a modifier for von Hippel-Lindau disease [16,17]. Exome sequencing also detected two heterozygous missense variants that were specific to group 1 (Table S1).

When all variants were included, exome sequencing revealed: (1) 83 non-synonymous and 86 synonymous variants that were present in groups 1+2 and absent from group 3 (Table S2); (2) 54 non-synonymous and 48 synonymous variants that were present in group 1 and absent from groups 2+3 (Table S3); (3) 6,033 non-synonymous and 6,667 synonymous variants that were present in groups 1+2, but not specific to groups 1+2 (thus, they may be present in group 3 or absent from group 3); and (4) 7,073 non-synonymous and 7,861 synonymous variants that were present in group 1, but not specific to group 1. Furthermore, comparison of the exome sequencing data between group 1 with hypocalcemia and group 2 without hypocalcemia revealed 231 non-synonymous and 254 synonymous variants that were present in group 1 and absent from group 2 (Table S4), and 246 non-synonymous and 242 synonymous variants that were present in group 2 and absent from group 1 (Table S5). (The variant data other than those described in Supplemental Tables may be available on request after discussion with the family members and approval by our IRBs, because they contain a huge amount of individual genetic information.)

In silico protein functional analysis

The results are summarized in Table S1. The p.G204R in *HDAC4* and the p.E276del in *CCND1* were assessed as non-pathologic, while some variants were evaluated as potentially pathologic.

Discussion

Exome sequencing successfully identified a heterozygous frameshift variant on exon 9C of *TBX1*. The c.1253delA (p.Y418fsX459) appears to be a disease-causing mutation, because it is predicted that this variant escapes nonsense-mediated mRNA decay due to its position on the final exon [18] and produces a truncated protein lacking the nuclear localization signal (NLS) and most of the transactivation domain (TAD) on exon 9C (Fig. 3) [19]. In support of this, functional studies for a similar c.1223delC (p.S408fsX459) mutation on exon 9C have shown that the truncated p.S408fsX459 protein was incapable of localizing to nucleus and lost transactivation function [2,5,19]. One may argue that this c.1253delA mutation affects *TBX1* isoform C (*TBX1C*, TBX1-003) alone, while *TBX1* produces three transcript variants containing T-box [2,4] (Fig. 3). However, *TBX1C* is the major transcript with the NLS and the TAD in human and is highly homologous to mouse *Tbx1* [4] (Fig. S1).

Craniofacial features in groups 1+2 and hypocalcemia in group 1 are well explained by the *TBX1* mutation [3]. This argues for a critical role of this mutation in the phenotypic development in groups 1+2, while the clinical effects of the remaining variants identified by exome sequencing are largely unknown. In this regard, comparison between group 1 with hypocalcemia and group 2 without hypocalcemia revealed a large number of non-synonymous and synonymous variants that exclusively belonged to either group 1 (Table S4) or group 2 (Table S5), although the lists did not contain a c.2968A>G (p.R990G) SNP in *CASR* (calcium sensing receptor) that has a gain-of-function effect and appears to raise the susceptibility to hypocalcemia (Fig. S2) [20]. Thus, it is

Table 1. Clinical findings of the family members.

	TBX1 mutation (+)					*TBX1* mutation (−)			*TBX1* mutation (N.E.)		
Individual	**II-2**	**III-1**	**III-5**	**III-6**	**III-7**	**II-1**	**III-3**	**IV-1**	**II-3**	**II-4**	**III-2**
Present age (year)	51	26	19	13	10	59	22	5	50	49	25
Sex	F	F	M	F	M	M	F	M	M	M	M
Craniofacial features	+	+	+	+	+	–	–	–	–	–	–
Hypertelorism	+	+	+	+	+	–	–	–	–	–	–
Blepharophimosis	+	+	+	+	+	–	–	–	–	–	–
Low set ears	+	+	+	+	+	–	–	–	–	–	–
Auricular anomalies	+	–	–	–	–	–	–	–	–	–	–
Narrow nose	+	+	+	+	+	–	–	–	–	–	–
Cleft palate	–	–	–	–	–	–	–	–	–	–	–
Micrognathia	±	+	+	+	+	–	–	–	–	–	–
Velopharyngeal incompetence	+[d]	+	+	+	+	–	–	–	–	–	–
Hypoparathyroidism	+	–	+	–	+	–	–	–	–	–	–
Age at examination (year)	44	17	8	4	0 (1 day)	N.E.	15	0 (6 days)	N.E.	N.E.	18
Serum calcium (mg/dL)[a]	7.6[e]	9.0	6.0	9.1	5.9	…	9.0	9.8	…	…	9.6
Serum i-phosphate (mg/dL)[a]	3.9[e]	4.9	9.1	5.0	N.E.	…	4.8	6.3	…	…	4.6
Serum intact PTH (pg/dL)[a]	31[e]	N.E.	15	N.E.	19	…	N.E.	34	…	…	N.E.
Cardiovascular anomalies[b]	–	–	–	–	–	–	–	–	–	–	–
Hypoplastic thymus[c]	–	N.E.	N.E.	N.E.	N.E.	N.E.	N.E.	N.E.	N.E.	N.E.	N.E.
Susceptible to infection	–	–	–[f]	–	–	–	–	–	–	–	–
Other features	–	–	–	–	–	–	–	–	–	–	–
Developmental retardation	+	+	+[g]	+	+[g]	–	–	–	–	–	–
Sensorineural deafness	+[h]	–	–	–	–	–	–	–	–	–	–
Graves' disease	–	–	+[i]	–	–	–	–	–	–	–	–

Individuals correspond to those shown in Fig. 1.
i-phosphate: inorganic phosphate; SD: standard deviation; F: female; M: male; and N.E.: not examined.
[a]Reference values: calcium, 9.0–11.0 mg/dL in infants and 8.8–10.2 mg/dL in adults; inorganic phosphate, 4.8–7.5 mg/dL in infants and 2.5–4.5 mg/dL in adults, and intact PTH, 10–65 pg/dL in infants and 14–55 pg/dL in adults.
Conversion factor to the SI unit: 0.25 for calcium (mmol/L), 0.32 for inorganic phosphate (mmol/L), and 0.106 for intact PTH (pmol/L).
[b]Examined by echocardiography, chest roentgenography, and/or electrocardiography.
[c]Examined by computed tomography.
[d]Received velopharyngeal closure.
[e]On treatment with vitamin D.
[f]Repeated otitis media only.
[g]Received speech therapy.
[h]Required hearing aids.
[i]At the time of diagnosis (11 years of age), serum TSH was <0.01 mIU/L, free T_3 33.1 pg/mL [51.0 pmol/L], free T_4 5.11 ng/dL [65.8 nmol/L], and TSH receptor antibody 1284% [normal range <1.9%].
doi:10.1371/journal.pone.0091598.t001

likely that, together with environmental factors, the combination of hitherto unknown calcium metabolism-related functional variants would underlie different serum calcium values between groups 1 and 2.

In addition to craniofacial features with and without hypocalcemia, *TBX1* mutation positive subject II-2 had sensorineural deafness, and III-5 had Graves' disease. Since such features are occasionally manifested by patients with 22q11.2DS [21,22], the results may suggest the relevance of *TBX1* to such rather infrequent features in 22q11.2DS.

The five *TBX1* mutation positive subjects in groups 1+2 lacked cardiovascular lesion and manifested borderline to mild developmental retardation (while they had no susceptibility to infection, assessment of thymic hypoplasia remained fragmentary). By contrast, cardiovascular lesion is frequently observed and developmental retardation is rare in previously reported patients with *TBX1* mutations, although clinical features are fairly variable among mutation positive patients (Table 2). Such difference would more or less be ascribed to an examination bias that *TBX1* has been analyzed in patients with isolated cardiovascular lesion in several studies [4,6,7] or to the functional difference of the mutant proteins [2,5–8]. However, in seven patients who have been examined for DGS/VCFS-like clinical features and found to have frameshift mutations on exon 9C (p.S408fsX459, p.H425fsX613, and p.S431fsX608) affecting the NLS and the TAD, cardiovascular lesion was present in four patients and developmental delay was absent or not described, despite apparent similarity in the ascertainment of patients and the function of mutant proteins between the seven patients and the five affected subjects in this family (Table 2) [2–5].

Thus, there may be protective factor(s) for cardiovascular lesion and susceptibility factor(s) for developmental delay in groups 1+2.

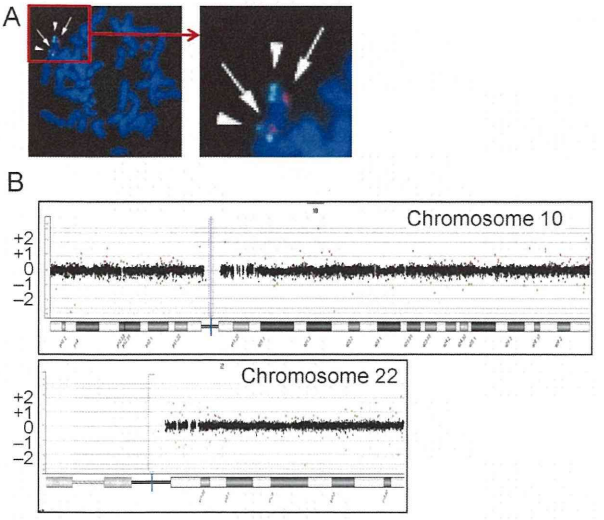

Figure 2. FISH and array CGH analyses in the proband (III-5). A. FISH analysis. Two signals are shown for both *HIRA* at 22q11.2 (red signals indicated by arrows) and *ARSA* at 22q13 (green signals indicated by arrowheads). **B.** Array CGH analysis. No copy number change is found for chromosome 10 carrying the second DiGeorge region and chromosome 22 harboring the DGS/VCFS critical region, as well as other chromosomes (not shown). Black, red, and green dots denote signals indicative of the normal, the increased (>+0.5), and the decreased (<−0.8) copy numbers, respectively. Although several red and green signals are seen, there is no portion associated with ≥3 consecutive red or green signals.
doi:10.1371/journal.pone.0091598.g002

In this regard, a simple explanation would be that protective factor(s) for cardiovascular lesion are present in groups 1+2 and may be present in group 3 or absent from group 3, whereas susceptibility factor(s) for developmental delay is present in groups 1+2 and absent from group 3. Since 6,033 non-synonymous and 6,667 synonymous variants were found to be present in groups 1+2 but not specific to groups 1+2, and 83 non-synonymous and 86 synonymous variants were revealed to be present in groups 1+2 and absent from group 3, a certain fraction of functional variants may constitute protective factor(s) for cardiovascular lesion and susceptibility factor(s) for developmental delay. In addition, while p.G204R on *HDAC4* for brachydactyly-mental retardation syndrome was assessed as non-pathologic by *in silico* analysis, it may have played a certain role in the occurrence of developmental delay in groups 1+2. Actually, such protective and susceptibility factor(s) would be more complex, with the effects of functional variants unique to each patient as well as the influences of environmental factors. Furthermore, it remains possible that the c.1253delA (p.Y418fsX459) mutation found in this study may be related to a specific phenotype characterized by the presence of craniofacial features and developmental delay and by the absence of cardiovascular lesion, because of a hitherto unrevealed mechanism(s). This matter awaits further studies.

Besides the clinical findings, several matters are also notable in the nine apparently pathologic *TBX1* mutations identified to date (Table 2). First, the mutations reside on exons 3–8 common to isoforms A–C or on exon 9C specific to isoform C, with no mutation on exons 9A and 9B specific to isoforms A and B. This would be consistent with *TBX1C* having the primary biological function. Second, while most mutations have loss-of-function effects, gain-of-function effects have been suggested for p.F148Y, p.H194Q, and p.310S by *in vitro* studies [8]. Thus, *TBX1* loss-of-function mutations and gain-of-function mutations may result in overlapping clinical features. Lastly, the c.1274_1281delACTATCTC (p.H425fsX613) missing the NLS on exon 9C was shared by a patient with DGS-like phenotype and the apparently normal mother, and the c.129_185del57 (p.43-61del19) with reduced transcriptional activity was common to a patient with non-syndromic tetralogy of Fallot and the apparently normal mother. This would imply the reduced penetrance of phenotypes caused by these mutations.

In summary, we identified a *TBX1* mutation by exome sequencing in a family with chromosome 22q11.2 deletion-like

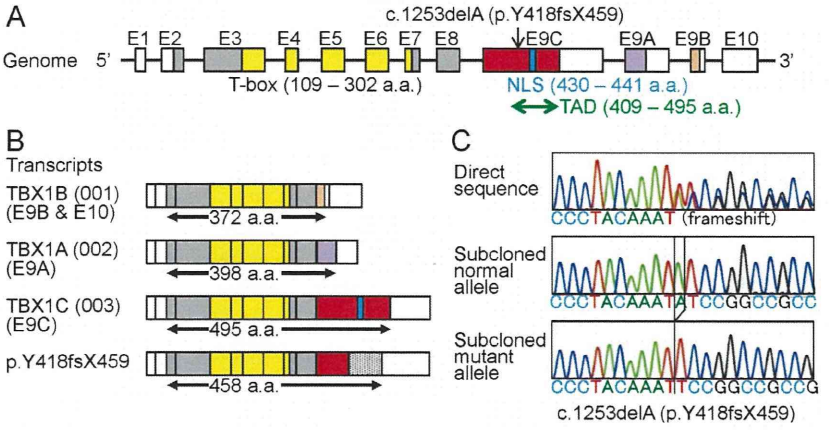

Figure 3. *TBX1* mutation identified in this family. A. Genomic structure of *TBX1* and the position of the mutation. The color and the white boxes represent the coding regions and the untranslated regions on exons 1–10 (E1–E10), respectively; the red, the purple, and the orange segments indicate the coding regions on the final exons 9C, 9A, and 9B (splice variants), respectively. The T-box is indicated by yellow boxes, the nuclear localization signal (NLA) by a blue segment, and the transactivation domain (TAD) by a green arrow. The c.1253delA (p.Y418fsX459) identified in this family resides on exon 9C. **B.** Transcripts of *TBX1*. Three variants are formed by alternative splicing of the final exons 9C, 9A, and 9B. The c.1253delA (p.Y418fsX459) mutation is predicted to yield a truncated TBX1C protein missing the NLS and most of the TAD. The stippled box of p.Y418fsX459 denotes aberrant amino acid sequence produced by the frameshift mutation. **C.** Electrochromatograms showing the frameshift mutation by Sanger sequencing. The primer sequences used are: 5′-GCGGCCAAGAGCCTTCTCT-3′ and 5′-GGGTGGTAGCCGTGGCCA-3′.
doi:10.1371/journal.pone.0091598.g003

Table 2. Summary of patients with *TBX1* mutations.

	TBX1C only					TBX1A–C				22q11.2DS
Position	**Exon 9C**	**Exon 9C**	**Exon 9C**	**Exon 9C**	**Exon 9C**	**Exon 3**	**Exon 4**	**Exon 5**	**Exon 8**	
cDNA change[a]	c.1223 delC	c.1253 delA	c.1274_1281 del8	c.1293_1315 del23[h]	c.1399_1428 dup30[k]	c.129_185 del57[k]	c.443T>A	c.582C>G	c.928G>A	Deletion
Amino acid change	p.S408 fsX459	p.Y418 fsX459	p.H425 fsX613	p.S431 fsX608	p.467_476 dup10A	p.43_61 del19	p.F148Y	p.H194Q	p.G310S	
NLS (exon 9C)	–	–	–	+[i]	+[i]	+	+	+	+	
TAD (exon 9C)	–	Involved	Involved	Involved	Involved	+	+	+	+	
Function	LOF	N.E.	N.E.	LOF	LOF	Reduced	GOF[m]	GOF[m]	GOF[m]	
Patient number	3	5	1	3[j]	2	1	1	2	1	558
Occurrence	Familial	Familial	Sporadic[g]	Familial	Sporadic	Sporadic[g]	Sporadic	Familial	Sporadic	
Facial features[b]	3/3	5/5	+	3/3	0/2	–	+	2/2	+	100%
Nasal voice[c]	2/3	5/5	N.D.	3/3	0/2	–	+	0/2	+	32%
Cardiovascular anomalies	1/3	0/5	+	2/3	2/2	+	+	0/2	+	57%
Hypopara-thyroidism[d]	1/3	3/5	+	N.D.	0/2	–	–	0/2	+	60%
Hypoplastic thymus	1/2[e]	0/1[f]	+	N.D.	0/2	–	–	N.E.	+	?
Susceptible to infection	N.D.	0/5	N.D.	N.D.	0/2	–	N.D.	N.D.	N.D.	?
Developmental retardation	0/3	5/5	N.D	0/3	0/2	–	–	1/2	–	38%
Reference	2	This study	3, 4	5	4, 6	7	2	8	2	1

In addition to the mutations listed in this table, several missense variants and in-frame indels with unknown functions have been found in patients with isolated cardiovascular anomalies and in those with DGS/VCFS-like phenotype [4].
NLS: nuclear localization signal; TAD: transactivation domain; LOF: loss-of-function; N.D.: not described; N.E.: not examined; GOF: gain-of-function; Del: deletion; and Dup: duplication.
[a]According to NM_080647.
[b]Suggestive of 22q11.2 deletion syndrome.
[c]Velopharygeal insufficiency.
[d]Hypocalcemia is included.
[e]Two of the three subjects have been examined for hypoplastic thymus.
[f]One of the five subjects has been examined for hypoplastic thymus.
[g]These two mutations have been inherited from apparently normal mothers.
[h]The c.1293-1315del23 has been described as c.1320-1342del23 in the original report [5].
[i]Although the natural NLS has been disrupted, a new NLS-compatible motif (RGRRRRCR) has been created on the added amino acid sequence.
[j]Another deceased individual in this family also has similar clinical features.
[k]These two mutations have been identified in *TBX1* analyses for patients with cardiovascular anomalies only.
[l]The mutant protein is aggregated in the cytoplasm and the nucleus.
[m]Gain-of-function effects have been found by *in vitro* studies [8].
doi:10.1371/journal.pone.0091598.t002

phenotype. Application of such powerful methods will serve to identify a causative gene in genetically heterogeneous disorders.

Supporting Information

Figure S1 Comparison of amino acid sequence of human *TBX1C* and mouse *Tbx1*. The T-box is highlighted in yellow, and the nuclear localization signal in light blue. The region for transactivation domain is surrounded by squares. The Y highlighted in red denotes the amino acid residue where the frameshift mutation in this family has taken place.
(TIF)

Figure S2 Analysis of c.2968A>G SNP (p.R990G, rs1042636) with a gain-of-function effect in exon 7 of *CASR*. The SNP pattern is not co-segregated with the presence or absence of hypocalcemia.
(TIF)

Table S1 Summary of heterozygous non-synonymous variants.
(PDF)

Table S2 A list of variants that are present in groups 1+2 and absent from group 3.
(PDF)

Table S3 A list of variants that are present in group 1 and absent from groups 2+3.
(PDF)